Changes in satellite cell content and myosin isoforms in low-frequency-stimulated fast muscle of hypothyroid rat

CHARLES T. PUTMAN, SABINE DÜSTERHÖFT, AND DIRK PETTE
Faculty of Biology, University of Constance, D-78457 Constance, Germany

Putman, Charles T., Sabine Düsterhöft, and Dirk Pette. Changes in satellite cell content and myosin isoforms in low-frequency-stimulated fast muscle of hypothyroid rat. *J. Appl. Physiol.* 86(1): 40–51, 1998.—Chronic low-frequency stimulation was used to study the effects of enhanced contractile activity on satellite cell content and myosin isoform expression in extensor digitorum longus muscles from hypothyroid rats. As verified by immunohistochemical staining for desmin, vimentin, and myosin heavy chain (MHC) isoforms and by histological analysis, stimulation induced a transformation of existing fast fibers toward slower fibers without signs of fiber deterioration or regeneration. Immunohistochemically detected increases in MHC I and MHC IIa isoforms, as well as reduced numbers of fibers expressing the faster MHC isoforms, mirrored the rearrangement of the thick-filament composition. These changes, especially the upregulation of MHC IIa, were accompanied by an induction of developmental MHC isoforms in the transforming adult fibers. Satellite cell content rose 2.6-, 3.0-, and 3.7-fold over that of corresponding controls ($P < 0.05$ in all cases) in 5-, 10-, and 20-day-stimulated muscles, respectively. Hypothyroidism alone had no effect on satellite cell content but resulted in a significant reduction in fiber size. The relative satellite cell contents increased ($P < 0.05$) from 3.8% in euthyroid control muscles to 7.9, 11.5, and 13.8% in the 5-, 10-, and 20-day-stimulated hypothyroid muscles, respectively. In 20-day-stimulated muscles, the relative satellite cell content reached an almost twofold higher level than that of normal slow-twitch soleus muscle. This increase occurred concomitantly with a rise in myonuclear density, most probably because of the fusion of satellite cells with existing fibers.

chronic low-frequency stimulation; developmental myosin; muscle fiber transformation; myosin heavy chain isoforms; satellite cell number

CHRONIC LOW-FREQUENCY STIMULATION (CLFS) of mammalian fast-twitch muscle has been shown to induce fast-to-slow fiber type transitions (see Refs. 18, 19 for reviews). The role of satellite cells in this transformation process has as yet not been elucidated. Satellite cells are quiescent myoblasts associated with adult fibers and represent the muscle fibers' regenerative, and possibly adaptive, potential. An involvement of satellite cells in fiber type conversions may be speculated, especially in light of recent evidence that fast and slow satellite cell lineages exist in mammalian fast and slow muscles, respectively (1, 7). Thus the possibility cannot be excluded that slow-type satellite cells are activated under the influence of CLFS and fuse to existing fast fibers. This might not only increase myonuclear content but might also evoke some reprogramming of muscle fiber phenotypes. Indeed, because fast muscles contain fewer satellite cells than do slow muscles (8), the induced fast-to-slow transformation can be expected to lead to an increase in satellite cell number. This notion is supported by the observation that cross-transplantation of fast and slow muscles alters the satellite cell content according to the properties of the host muscle bed (25). Similarly, altered functional demands such as exercise, stretch, or immobilization have been shown to alter the mitotic activity and/or content of satellite cells (4, 26, 27, 30).

Pronounced satellite cell proliferation has previously been shown in electrically stimulated rabbit muscle (16, 24). However, because ongoing fiber degeneration and regeneration accompanied the fast-to-slow fiber type conversion in rabbit muscle, it was concluded that the role of satellite cells was to replace degenerating fibers (16, 24). In contrast, CLFS-induced fiber type transitions in rat muscle occur seemingly independent of degeneration/regeneration processes (5). Therefore, rat muscle appeared to be an appropriate model to study the behavior of satellite cells in response to CLFS.

The purpose of the present study was to investigate the time course of changes in satellite cell content during CLFS-induced fast-to-slow fiber type transitions of hypothyroid rat muscle. Hypothyroidism was chosen because it has been shown that the restricted plasticity of rat muscle can be overcome, to some extent, by reducing the thyroid hormone level (13). Changes in satellite cell number, muscle fiber morphology, and fiber types were examined. Satellite cells were identified by their location between the basal lamina and the sarcolemma by using the method of triple staining of laminin, dystrophin, and nuclear staining by hematoxylin (36). Muscle-fiber morphology was assessed by histological analyses and by immunohistochemical staining of desmin and vimentin to identify regenerating fibers (2, 9). Muscle fiber type transitions were characterized immunohistochemically and electrophoretically, according their adult myosin heavy chain (MHC) composition.

MATERIALS AND METHODS

Animals and hypothyroidism. Twenty-eight adult (4-mo-old) male Wistar rats (Thomae, Biberach, Germany) were utilized in this study. All animal experiments were approved by the local government (Regierungspräsidium Freiburg). The rats were treated in accordance with established principles of care and use. They were housed in the Animal Research Center of the University of Constance in a thermally controlled room maintained at 22°C with 12:12-h dark-light cycles. Before stimulation was initiated, hypothyroidism was induced in 23 rats by 7 wk of feeding an

The costs of publication of this article were defrayed in part by the payment of page charges. The article must therefore be hereby marked "*advertisement*" in accordance with 18 U.S.C. Section 1734 solely to indicate this fact.

 8750-7587/99 $5.00 Copyright © 1999 the American Physiological Society

iodine-poor diet (Altromin C1042, Altromin, Lage, Germany) and by the addition of propylthiouracil to the drinking water. The remaining five euthyroid controls received a regular diet (Altromin 1314). The euthyroid rats weighed 489 ± 28 (SD) g at the beginning of CLFS and gained 13 ± 6 g over the course of the experiment. The hypothyroid rats weighed 308 ± 7 g at the beginning of CLFS and lost 46 ± 24 g during 20 days of CLFS. The extensor digitorum longus (EDL) muscles of the euthyroid rats weighed 219 ± 29 mg and the hypothyroid EDL muscles 129 ± 13 mg. In all groups, there were no differences between left and right EDL muscles.

CLFS and muscle sampling. Electrodes were implanted laterally to the peroneal nerve of the left hindlimb (28). After 1 wk of recovery, stimulation was started (continuously for 10 h/day at 10 Hz, impulse width 0.3 ms). The following groups were studied: 0-day-stimulated euthyroid controls ($n = 5$); 0-day-stimulated hypothyroid controls ($n = 5$), and 5- ($n = 5$), 10- ($n = 7$), and 20-day-stimulated ($n = 6$) hypothyroid animals. The left leg of the 0-day-stimulated animals was sham operated. After stimulation, rats were euthanized, and the EDL muscles of the stimulated (left) and contralateral control (right) legs were excised, weighed, and frozen in melting (−159°C) isopentane. Muscles were stored in liquid nitrogen until analyzed.

Antibodies. Anti-dystrophin monoclonal antibodies (MAb) directed against the mid-rod domain (DYS1), the COOH terminal (DYS2), and the NH_2 terminal domain (DYS3), and antidevelopmental MHC (MHC_{dev}) antibody (clone NCL-D) were obtained from Novocastra Laboratories (Newcastle, UK). Polyclonal and monoclonal anti-laminin was obtained from ICN Biomedicals (Costa Mesa, CA). To examine changes in fiber type distribution, the following MAbs directed against adult MHC isoforms were used: MHC I (BA-D5), MHC IIa (SC-71), and MHC IId/x/IIb (BA-D9) (22). Monoclonal anti-desmin (clone DE-B-5) and monoclonal anti-vimentin (clone V9) were obtained from Boehringer Mannheim. Biotinylated horse anti-mouse IgG (rat absorbed, affinity purified) and biotinylated goat anti-rabbit IgG were obtained from Vector Laboratories (Burlingame, CA). Alkaline phosphatase-conjugated goat anti-mouse IgG and peroxidase-conjugated goat anti-rat IgG were obtained from Dianova (Hamburg, Germany).

Immunohistochemistry for identification of satellite cells. Satellite cells were localized immunohistochemically according to their location between the basal lamina and the sarcolemma, as previously described (36). Freshly cut frozen sections (5 and 9 μm thick) were air-dried for 2 h at room temperature and fixed in cold acetone (−20°C) for 10 min. Sections were washed once in PBS-Tween (0.1% vol/vol), twice in PBS, and then incubated for 30 min in a solution of 3% H_2O_2 in methanol. Sections were washed as before and incubated for 1 h in a blocking solution (BS-1) (1% BSA, 10% goat serum, and 0.1% Tween-20 in PBS, pH 7.4). Excess blocking solution was removed, and polyclonal anti-laminin diluted (1:300) in BS-1 was overlaid and incubated at 4°C overnight. Sections were washed as before and incubated with biotinylated goat anti-rabbit IgG (30 min), washed and incubated with a biotin-avidin-horseradish peroxidase complex (Vectastain Elite, Vector Laboratories) for 30 min. Sections were then washed and reacted with a peroxidase substrate solution: 0.016% 3-amino-9-ethyl-carbazole and 0.06% H_2O_2 in a 50 mM acetate buffer (pH 5.0) (Immunotech, Hamburg, Germany). The reaction was stopped by repeated washings in PBS, after which a mixture of DYS1, DYS2, and DYS3, each diluted 1:8 in BS-1, was overlaid and incubated overnight at 4°C. Sections were washed and incubated for 1 h at 37°C with alkaline phosphatase-conjugated goat anti-mouse IgG diluted in BS-1 (1:2,000). Sections were washed again and incubated for 15 min with an alkaline phosphatase substrate solution: 0.03% nitroblue tetrazolium, 0.002% 5-bromo-4-chloro-3-indolyl phosphate, 100 mM NaCl, 50 mM $MgCl_2$, and 100 mM Tris, pH 9.5. The reaction was stopped by washing the samples several times in PBS. Sections were then rinsed in distilled water, counterstained with Mayer's Hemalum (Merck, Darmstadt, Germany), and mounted with GelTol aqueous mounting medium (Immunotech). On some sections, polyclonal anti-laminin and goat anti-rabbit IgG were substituted with monoclonal anti-laminin and peroxidase-conjugated goat anti-rat IgG, respectively. Negative controls with omission of the primary antibodies were simultaneously incubated in BS-1.

Immunohistochemistry for myosin, desmin, and vimentin. Nine-micrometers-thick frozen sections were air-dried, washed once in PBS-Tween, twice in PBS, and incubated for 30 min in 3% H_2O_2 in methanol. Sections were subsequently washed and incubated for 1 h in BS-2 (1% BSA, 10% horse serum, and 0.1% Tween-20 in PBS, pH 7.4). Excess blocking solution was removed, and the primary MAb was overlaid and incubated overnight at 4°C. Primary antibodies were diluted in BS-2 as follows: MHC_{dev} (NCL-D), 1:50; MHC I (BA-D5), 10 μg/ml; MHC IIa (SC-71), 10 μg/ml; MHC IId/x/IIb (BA-D9), 10 μg/ml; desmin, 4 μg/ml; and vimentin, 2.5 μg/ml. Sections were washed and reacted for 30 min with biotinylated horse anti-mouse IgG. Sections were then washed, incubated with biotin-avidin-horseradish peroxidase complex for 30 min, washed again, and reacted for 6 min with a peroxidase substrate solution: 0.07% diaminobenzidine, 0.05% H_2O_2, and 0.03% $NiCl_2$ in 50 mM Tris (pH 7.5). In the case of desmin staining, $NiCl_2$ was omitted from the substrate solution. The reaction was stopped by washing several times with distilled water. Corresponding negative controls were simultaneously incubated in BS-2. Sections were subsequently dehydrated, cleared, and mounted in Entellan (Merck, Darmstadt, Germany).

Electrophoretic analysis of MHC isoforms. The MHC composition was examined as previously described (32). Briefly, SDS-PAGE gradient gels (5–8%) were prepared. Electrophoresis was run for 20 h at 12°C at 22 mA. Gels were silver stained, and the relative myosin composition was evaluated densitometrically. Electrophoretic analyses were only conducted on the euthyroid ($n = 3$) and hypothyroid control ($n = 3$) muscles and on 20-day-stimulated hypothyroid muscles ($n = 3$) to further characterize the full extent of the fast-to-slow fiber type transition.

Satellite cell number, fiber type, and cross-sectional area analyses. Satellite cells were identified as hematoxylin-stained nuclei located between the red-stained basal lamina and the black-stained plasma membrane, according to the criteria discussed in the original publication of the method (36). One set of 5-μm-thick and another set of 9-μm-thick sections were analyzed at ×1,250 magnification for each of the hypothyroid muscles, and the data were averaged. For the euthyroid control muscles, 9-μm-thick sections were analyzed. For each hypothyroid muscle, an average total area of $6.4 \pm 1.7 \times 10^5$ μm^2, corresponding to ~383 ± 92 fibers, was examined, amounting to 3.2 mm^2 for the five muscles or 1,915 fibers at each time point. For each euthyroid muscle, an average total area of $4.6 \pm 0.9 \times 10^5$ μm^2, corresponding to 146 ± 21 fibers, was examined, amounting to 2.4 mm^2 for the five muscles or 724 fibers for each of the two conditions. Satellite cell number and intrafiber myonuclei were evaluated per unit area. This appeared meaningful, as changes in fiber size were observed only with hypothyroidism, but no further changes occurred with CLFS (see Figs. 4 and 5).

Serial sections, stained for the various MHC isoforms, were examined to determine muscle fiber type and cross-sectional area, using a computer program. Briefly, video images were transferred to a computer monitor, fibers were circled with a computer mouse, and the enclosed area was integrated to determine fiber size. Approximately 200 fibers were evaluated for each muscle. Total intrafiber myonuclei were evaluated for each muscle on several (2–7) 9-μm-thick serial sections stained with nuclear fast red (Sigma Chemical, St. Louis, MO), and one set was stained with hematoxylin. A mean area of $8.2 \pm 2.1 \times 10^5$ μm^2 was evaluated for each muscle. Thus a total area of 4.1 mm^2 was examined for the five muscles studied at each time point for both the stimulated, sham, and control legs.

Statistical analyses. Data are presented as means ± SD. All data were analyzed by using two-way ANOVA with repeated measures within animals (control vs. stimulated or sham), except where indicated. Densitometric results of MHC gels were evaluated by one-way ANOVA. When a significant *F*-ratio was found, differences were located by using the Newman-Keuls post hoc analysis. Differences were considered significant at $P < 0.05$.

RESULTS

CLFS increases the total number of nuclei in the absence of morphological signs of muscle fiber degeneration/regeneration. Gross morphological signs of fiber regeneration were absent in stimulated muscles. As revealed by inspection of hematoxylin and eosin-stained cross sections (Fig. 1), as well as by acid phosphatase-stained sections (results not shown), there seemed to be no increase in mononucleated cells in the interstitium. The frequency of small fibers with centrally located nuclei was low (<1%) in stimulated muscles and was not elevated over euthyroid and hypothyroid controls (Fig. 1). Further examination of the immunohistochemical patterns of desmin and vimentin expression (Fig. 2) revealed that stimulated muscles stained more intensely for desmin. However, the intrafiber pattern of desmin staining was uniform. No conspicuous differences existed between stimulated and control muscles with regard to the incidence of

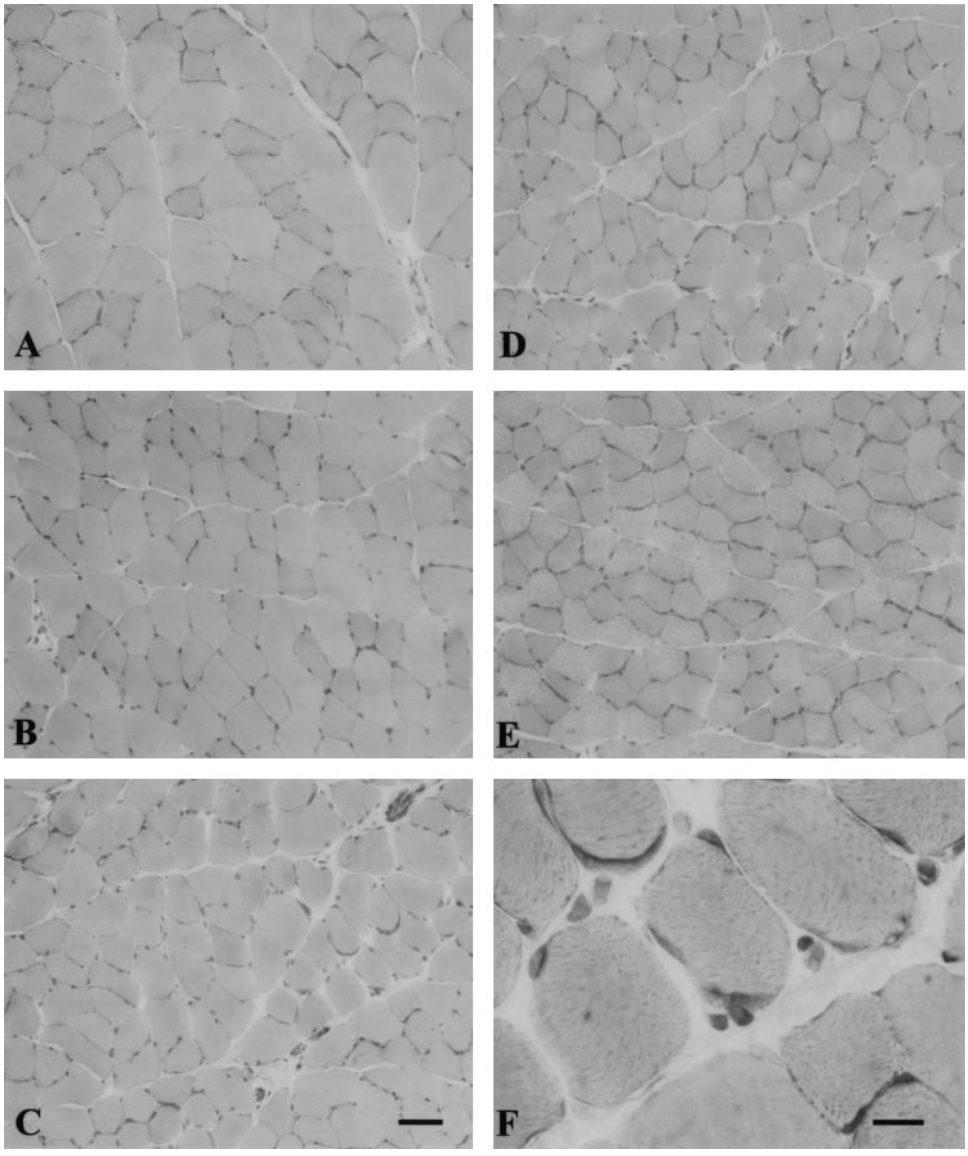

Fig. 1. Representative hematoxylin and eosin stains of euthyroid (*A*) and hypothyroid (*B*) control muscles, and of 5- (*C, F*), 10- (*D*), and 20-day-stimulated (*E*) hypothyroid extensor digitorum longus muscles of rat. Note absence of regenerating fibers, i.e., small fibers with central nuclei (*A-E*). Detaching nuclei (*F*) were commonly observed in stimulated muscles. Bar in *C*: 50 μm; bar in *F*: 15 μm.

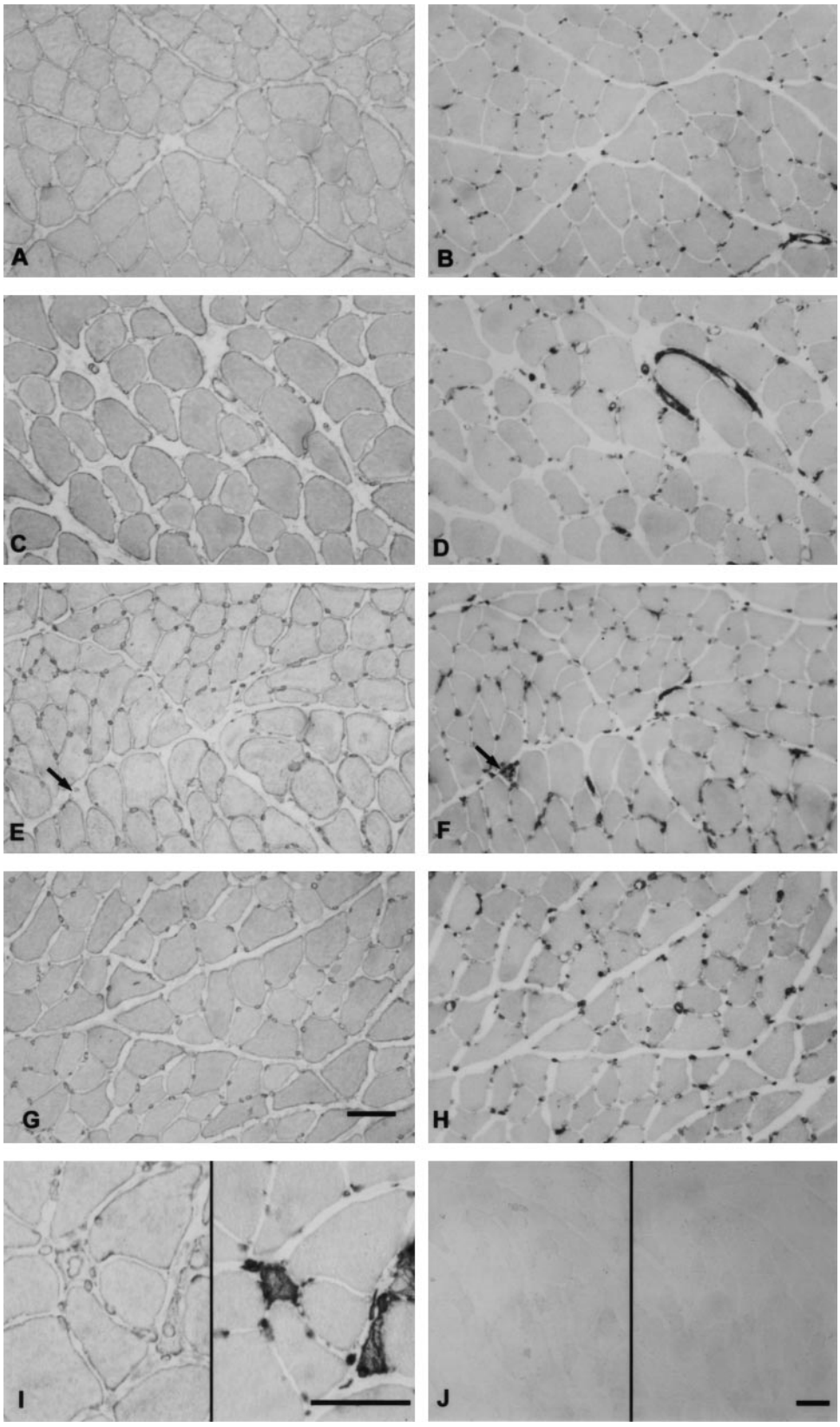

Fig. 2. Representative desmin (*A, C, E, G*) and vimentin (*B, D, F, H*) stains of hypothyroid control (*A, B*) and of 5- (*C, D*), 10- (*E, F*), and 20-day-stimulated (*G, H*) hypothyroid extensor digitorum longus muscles. Examples of regenerating fibers displaying foci of desmin reactivity (*left*) and induction of vimentin (*right*) are shown in *I*. Arrows point to another example of a regenerating fiber showing absence of desmin staining (*E*) and positive vimentin staining (*F*). In *J*, negative controls for desmin (*left*) and vimentin (*right*) without primary antibodies are shown. Note absence of these indicators of fiber regeneration in *A-H*. All bars are 50 μm.

fibers displaying either foci of desmin reactivity and/or regions devoid of desmin staining but re-expressing vimentin (see Fig. 2). By using this characteristic pattern of desmin and vimentin expression as a criterion to identify regenerating fibers (2, 9), all stimulated, sham, and contralateral control legs from the hypothyroid groups were examined. In the 46 muscles examined, a total of only 8 regenerating fibers was

positively identified: 4 in control, 1 in 5-day-stimulated, 2 in 10-day-stimulated, and 1 in 20-day-stimulated muscles. Enhanced vimentin expression was observed in stimulated muscles, but staining was restricted to blood vessels, the extracellular space, and some muscle nuclei (Fig. 2). Thus, in the present study, there were no obvious gross morphological signs of muscle fiber degeneration or regeneration.

Hypothyroidism as well as CLFS led to increases in the number of intrafiber nuclei expressed per square millimeter (Fig. 3). Hypothyroidism resulted in an ~50% increase in nuclear number. However, this increase was artifactual and could be wholly accounted for by a 50% decrease in mean fiber area (Fig. 4). The major decrease in mean fiber area was attributed to a 50% decrease in the fast fiber populations, whereas the decrease in the type I fibers amounted to only 20% (Fig. 5). Twenty days of CLFS resulted in a further 1.3-fold increase in intrafiber nuclear number (Fig. 3). However, unlike the effect of hypothyroidism, CLFS had no effect on fiber area (Figs. 4 and 5). Thus the increase in intrafiber nuclei of stimulated muscle resulted from enhanced neuromuscular activity.

Changes in satellite cell content. Satellite cells were identified according to the method of Zhang and McLennan (36). This method makes it possible to identify satellite cells at the light-microscopic level. Typical examples of hematoxylin-stained satellite cell nuclei between the laminin-stained basal lamina and the dystrophin-stained sarcolemma are shown in Fig. 6. This method proved to be equally applicable to all control (Fig. 6*A*) and experimental (Fig. 6*B*) muscles.

Quantitative evaluation of satellite cell stains under all experimental conditions revealed that hypothyroidism resulted in a 1.6-fold increase in the number of satellite cells per unit area (Fig. 7). However, this increase could also be entirely accounted for by the corresponding decrease in fiber area (Fig. 4). Conversely, CLFS markedly increased the absolute number of satellite cells (Fig. 7) as well as the relative satellite

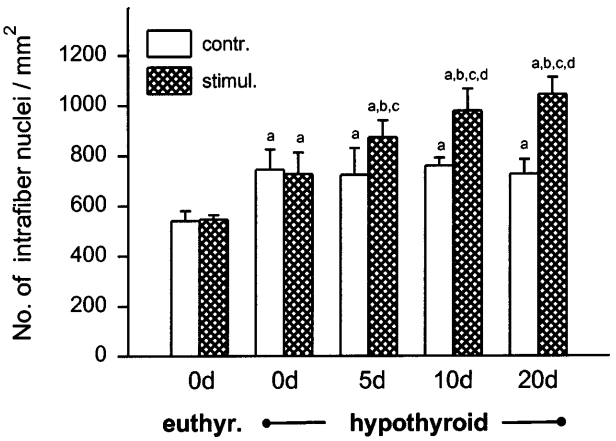

Fig. 3. No. of intrafiber muscle nuclei per square millimeter. Contr, contralateral control; Stimul, stimulated in the 5-, 10-, and 20-day groups; euthyr, euthyroid; d, day. The 0-day-stimulated animals were sham operated. [a]Different from euthyroid control; [b]different from hypothyroid control; [c]different from contralateral control; [d]different from 5-day-stimulated animals ($P < 0.05$).

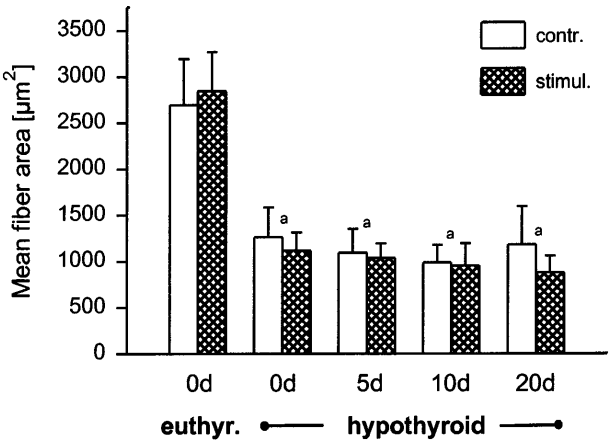

Fig. 4. Mean fiber area in stimulated and control muscles. [a]Different from euthyroid control ($P < 0.05$).

cell content (Fig. 8). After 5 days of stimulation, the number of satellite cells was elevated 2.6-fold (Fig. 7). Increases continued with longer periods of CLFS, reaching threefold and 3.7-fold elevations after 10 and 20 days over contralateral controls, respectively. As shown in Fig. 8, the major increase in satellite cells occurred during the first 10 days. The relative satellite cell content rose from 3.8% in the control to 7.9, 11.5, and

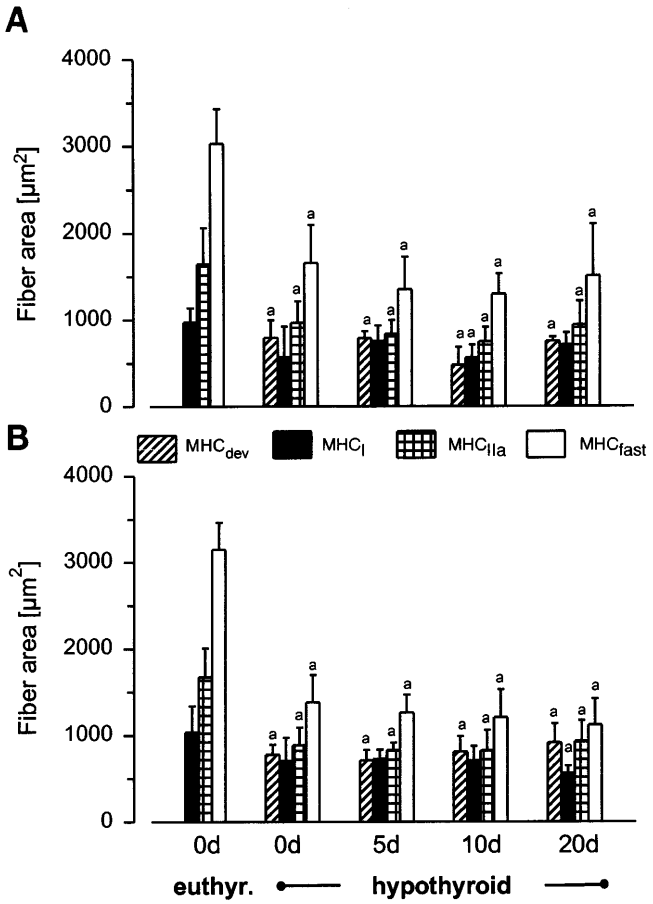

Fig. 5. Mean fiber areas of different fiber types in stimulated (*A*) and control muscles (*B*). MHC_{dev}, MHC I, MHC IIa, MHC_{fast}, myosin heavy chain isoforms. [a]Different from euthyroid control ($P < 0.05$).

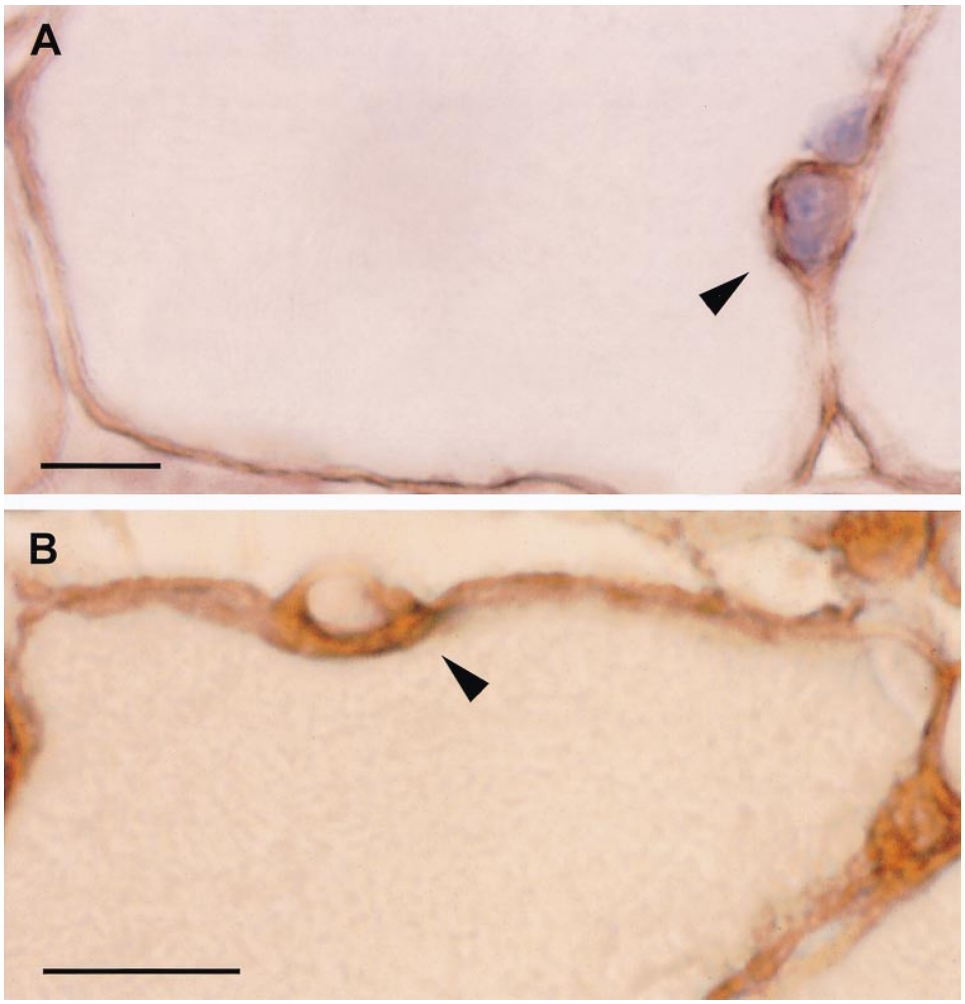

Fig. 6. Representative pictures of a stain used to identify satellite cells based on their location between basal lamina and sarcolemma. Inner sarcolemma is stained dark blue (anti-dystrophin). Outer basal lamina is stained red (anti-laminin), and nuclei are counterstained with Mayer's Hemalum. *A*: euthyroid control; *B*: hypothyroid control. Arrowheads indicate satellite cells located next to a myonucleus. Bar: 10 µm.

13.8% after 5, 10, and 20 days of CLFS, respectively. Referred to the contralateral controls, the average daily increase amounted to 0.82%/day during the initial period of CLFS. Subsequent increases occurred at a lower rate, with daily increments of ~0.65% between 5 and 10 days, and 0.42% between 10 and 20 days.

MHC isoforms and fiber type transitions. The expression of various MHC isoforms was studied immunohistochemically. Hypothyroidism induced the expression of MHC_{dev} and increased the proportion of MHC IIa- and MHC I-expressing fibers (Fig. 9; see also Fig. 11).

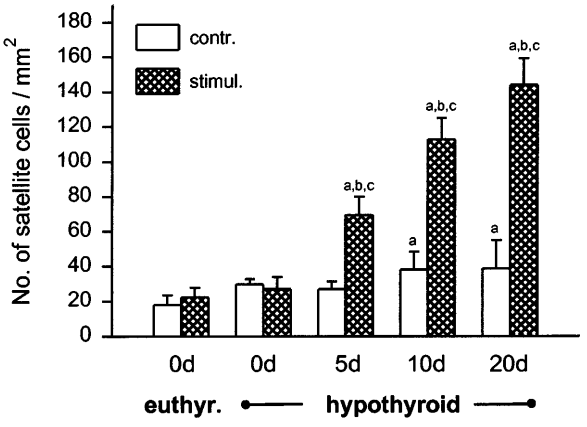

Fig. 7. No. of satellite cells per unit area in control and stimulated muscles. [a] Different from euthyroid control; [b] different from hypothyroid control; [c] different from contralateral control ($P < 0.05$).

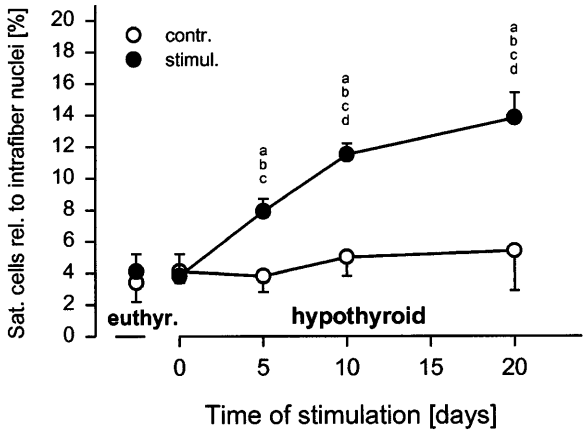

Fig. 8. Relative increase in satellite (Sat) cell content as a function of time of stimulation. rel, Relative. [a] Different from euthyroid control; [b] different from hypothyroid control; [c] different from contralateral control; [d] different from 5-day-stimulated animals ($P < 0.05$).

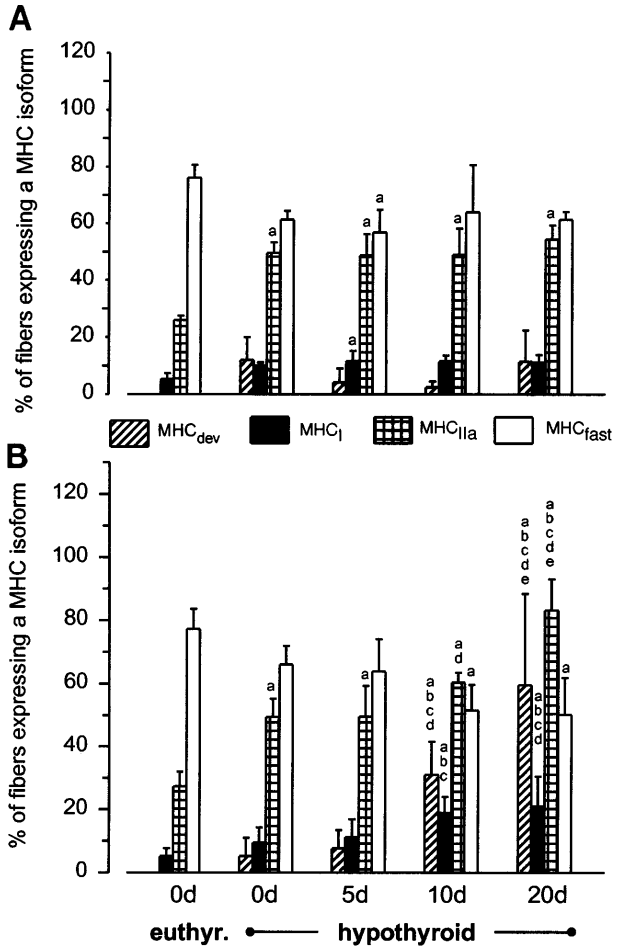

Fig. 9. Percentage of fibers immunoreactive for specific MHC isoforms in response to hypothyroidism (*A*) and duration of chronic low-frequency stimulation (CLFS; *B*). [a]Different from euthyroid control; [b]different from hypothyroid control; [c]different from contralateral control; [d]different from 5-day-stimulated animals; [e]different from 10-day-stimulated muscles ($P < 0.05$).

The proportion of fibers expressing one or both of the "fastest" isoforms, MHC IIb and MHC IId/x, was slightly reduced by hypothyroidism. As revealed by immunohistochemistry, major changes in the MHC isoform pattern were induced by CLFS and were characterized by pronounced increases in MHC I, MHC IIa, and MHC$_{dev}$ and a decrease in the proportion of fibers expressing the fast MHC IId/x and/or MHC IIb isoforms (MHC$_{fast}$) (Fig. 9). After 20 days, the proportion of these fast fibers was reduced by ~35%. A conspicuous finding was a significant increase in the expression of MHC$_{dev}$ in muscles stimulated >5 days. In 20-day-stimulated muscle, 60% of the fibers were strongly positive for MHC$_{dev}$. This MHC isoform had originally been included in our study to detect regenerating fibers. However, no such fibers were observed (see also Figs. 1 and 2) in the stimulated muscles, and, therefore, the strong reactivity of a major fiber fraction for MHC$_{dev}$ appeared to represent an important step in the adaptation process encompassing the fast-to-slow fiber type transformation.

As a consequence of the increased expression of MHC IIa and MHC I and the induction of MHC$_{dev}$, the population of hybrid fibers expressing more than a single MHC isoform increased (Fig. 10). Hypothyroidism caused a threefold increase in the proportion of hybrid fibers from 6 to 25%. CLFS further expanded the hybrid fiber population to 45 and 77% in 10- and 20-day-stimulated muscles, respectively (Fig. 10).

An interesting observation was the coexpression of MHC$_{dev}$ and adult MHC isoforms (Fig. 11, Table 1). During the first 10 days of CLFS, MHC$_{dev}$ was coexpressed with MHC IIa and/or MHC I (Fig. 11; Table 1). After 20 days of CLFS, the frequency of fibers expressing MHC$_{dev}$ with MHC IIa and/or MHC I remained stable, whereas the proportion of fibers coexpressing MHC$_{dev}$ with the two fast MHC IId/x and MHC IIb isoforms increased significantly (Fig. 11; Table 1).

Changes in immunohistochemically classified fiber types (Fig. 9; Table 1) corresponded to similar changes in the electrophoretically determined adult MHC isoforms (Fig. 12). MHC I increased from ~5.7% in the euthyroid and hypothyroid control muscles to 13.4% after 20 days of CLFS. The relative content of MHC IIa increased from 19.6 to 23.8% after 7 wk of hypothyroidism and to 33.5% after 20 days of stimulation. In contrast, MHC IId/x content did not significantly change and was 30% in euthyroid, 27% after 7 wk of hypothyroidism, and 26% after 20 days of CLFS. The largest single change occurred in the expression of MHC IIb, which was reduced from 44.8 to 24.9% in the 20-day-stimulated muscles.

DISCUSSION

The present study investigates effects of CLFS on satellite cells in rat fast-twitch muscle during the induced fast-to-slow fiber-type transition. Rat muscle is a highly suitable model because, due to the absence of gross morphological signs of fiber degeneration, the effects of CLFS on satellite cells can be studied in intact muscle fibers. Contrary to the rabbit where, in addition to fiber transformation, replacement of degenerating fibers by newly formed slow myotubes contributes to the stimulation-induced muscle conversion (16, 24), the

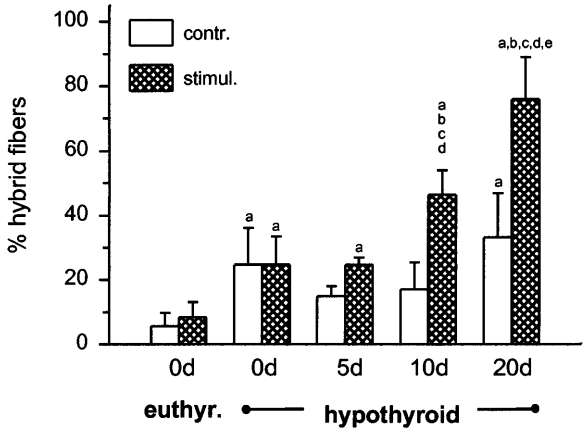

Fig. 10. Increase in proportion of hybrid fibers in response to hypothyroidism and duration of CLFS. [a]Different from euthyroid control; [b]different from hypothyroid control; [c]different from contralateral control; [d]different from 5-day-stimulated animals; [e]different from 10-day-stimulated muscles ($P < 0.05$).

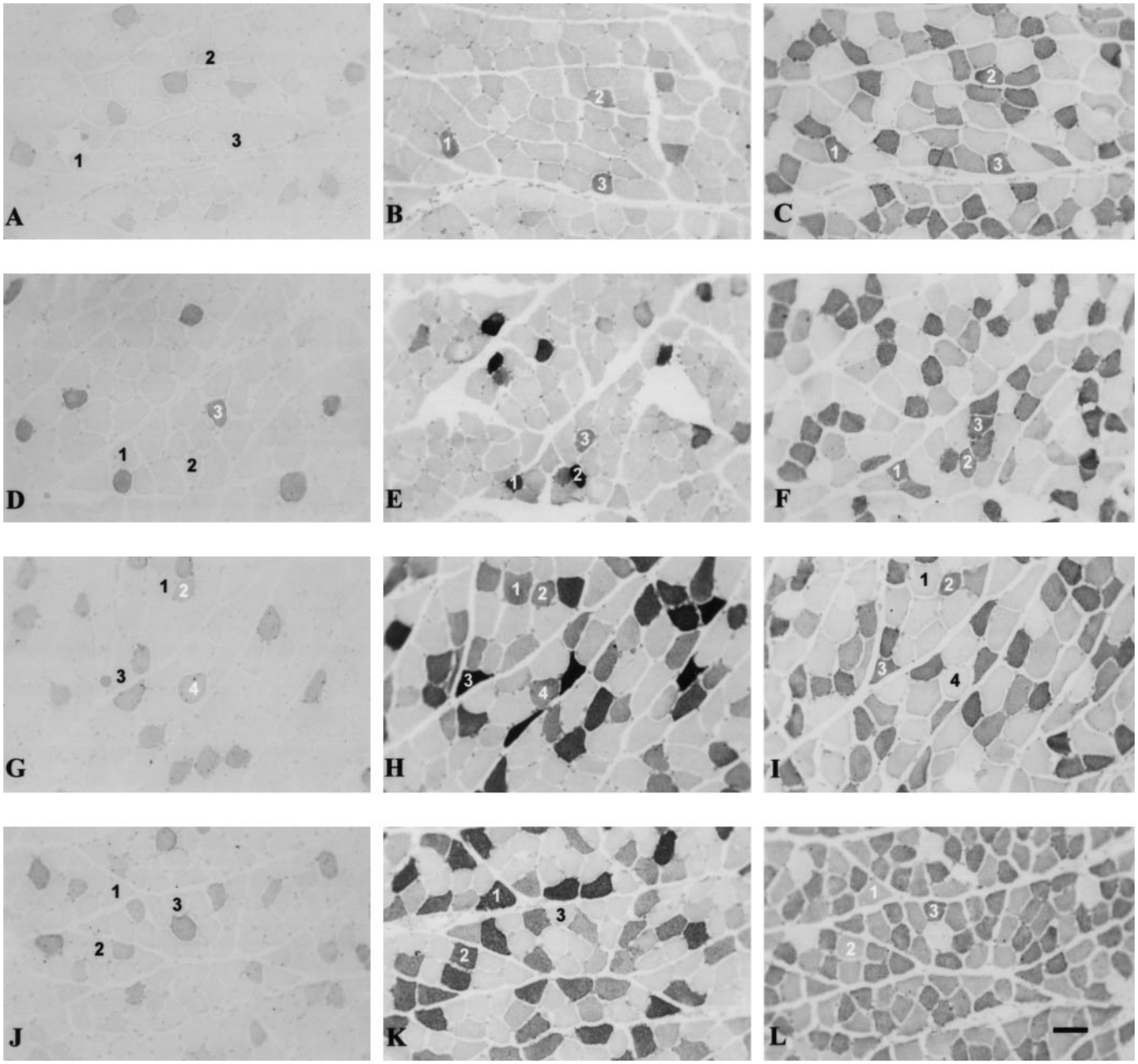

Fig. 11. Representative pictures of MHC immunostains in 0- (*A-C*), 5- (*D-F*), 10- (*G-I*), and 20-day-stimulated (*J-L*) hypothyroid rat extensor digitorum longus muscles. *A, D, G, J*: immunostains for MHC I with monoclonal antibody (MAb) BA-D5. *B, E, H, K*: immunostains for MHC_{dev} with MAb NCL-D. *C, F, I, L*: immunostains for MHC IIa with MAb SC-71. Note that immunoreactivity for MHC_{dev} is restricted to MHC I- and/or MHC IIa-positive fibers in the 0-day (*fibers 1, 2,* and *3*) and 5-day (*fibers 1, 2,* and *3*) groups. In the 10-day group, MHC_{dev} expression was detected in MHC I-positive (*fibers 2* and *4*) and MHC IIa-positive (*fibers 2* and *3*) fibers and also in fast fibers (*fiber 1*). Some fibers expressed all 3 isoforms (*fiber 2*). In the 20-day group, staining for MHC_{dev} is seen also in hybrid fibers (*fibers 1* and *2*) displaying immunoreactivity for MHC_{fast} and MHC IIa. Bar: 50 μm.

fast-to-slow transitions can be studied in rat muscle without degeneration/regeneration processes and thus can be considered to be exclusively brought about by the transformation of existing fibers. On the other hand, rat fast-twitch muscle is more resistant to the CLFS-induced transformation process than is rabbit muscle (5, 12, 32). As previously shown (13) and as confirmed by the present study, this resistance can be overcome by lowering the thyroid hormone level.

Muscle morphology. Compared with euthyroid and hypothyroid controls, muscles exposed to CLFS show no evidence of invasion by mononucleated cells. In addition, the absence of small myotubes and fibers with central nuclei in control and stimulated muscles excludes processes of fiber regeneration. The 20 and 50% reductions in the cross-sectional areas of type I and type II fibers, respectively, does not appear to result from regenerative events but, rather, from a reduction

Table 1. *Changes in MHC-based fiber types induced by hypothyroidism and chronic low-frequency electrical stimulation in rat EDL muscle*

		%Fiber Type								
Condition	Leg	I	I/IIa	Dev/I	Dev/I/IIa	Dev/IIa	IIa	IIa/Fast	Dev/IIa/Fast	Fast
Euthyroid	Sham	4.9±2.2	0.3±0.6	0.0±0.0	0.0±0.0	0.0±0.0	19.2±5.7	8.2±4.6	0.0±0.0	67.4±4.8
	Control	5.1±2.0	0.3±0.5	0.0±0.0	0.0±0.0	0.0±0.0	20.6±4.5	5.3±4.0	0.0±0.0	68.6±2.9
0-day	Sham	8.2±4.4	0.7±0.2	0.3±0.3	0.2±0.3	4.8±4.3	26.5±5.7	17.6±7.0	1.0±1.0	40.7±8.9[a]
	Control	7.5±1.9	1.8±1.9	0.3±0.3	0.4±0.4	10.5±7.5	26.9±5.0	11.0±3.5	0.9±0.7	40.7±4.2[a]
5-day	Stimulated	8.2±2.8	1.1±1.7	0.8±1.3	0.3±0.7	6.3±6.0	28.3±9.5	15.6±5.7	0.5±0.9	38.7±6.5[a]
	Control	10.5±3.4	0.4±0.5	0.7±0.7	0.2±0.4	2.0±2.3	34.9±8.0	10.4±3.3	1.3±2.1	39.7±5.0[a]
10-day	Stimulated	6.6±3.1	1.3±1.4	4.6±2.5[a,b,c,d]	6.4±3.4[a,b,c,d]	14.5±7.8[a]	19.8±10.5	14.1±7.4	5.5±3.5	27.1±3.1[a,b,c,d]
	Control	9.3±2.4	1.7±1.8	0.3±0.5	0.3±0.5	1.7±1.5	34.0±7.1	12.9±5.2	0.1±0.2	39.7±10.6*
20-day	Stimulated	10.0±6.5	3.8±4.8	0.5±0.6	6.8±5.8[a,b,c,d]	17.8±14.9[a,b]	11.6±11.6[b,c,d]	12.6±15.0	34.5±15.2[a,b,c,d]	2.3±5.2[a,b,c,d,e]
	Control	6.5±2.7	4.0±3.3	0.5±0.8	0.2±0.4	9.4±8.3	25.6±7.8	17.7±4.8	1.5±3.0	34.5±5.2[a]

Data are means ± SD, expressed as %total muscle fiber types. Fast, fibers expressing myosin heavy chain (MHC) MHC IId/x and/or MHC IIb isoforms. See text for further fiber-type description. EDL, extensor digitorum longus. [a] Different from euthyroid control; [b] different from hypothyroid 0-day control; [c] different from contralateral control; [d] different from 5-day hypothyroid; [e] different from 10-day hypothyroid.

in the net rate of protein synthesis related to the hypothyroid state (3). Similar effects of hypothyroidism on the cross-sectional area of rat muscle fibers have been reported by others (e.g., Ref. 17).

To further assess muscle-fiber integrity, the appearance of the exosarcomeric cytoskeletal architecture was studied by examining desmin and vimentin distribution patterns. Muscle-fiber damage typically results in disruption of the exosarcomeric cytoskeleton, followed by enhanced degradation of desmin, a major component of Z-discs. At the light-microscopic level, this can be detected immunohistochemically as a loss of desmin staining and/or as foci of intense desmin reactivity. In addition, the subsequent induction of vimentin creates a characteristic pattern of abnormal desmin staining combined with strong reactivity for vimentin in the same fiber (Fig. 2). These criteria have been used to identify degenerating/regenerating fibers in response to experimentally induced muscle injury (2, 33). In the present study, such patterns of desmin and vimentin distribution are rarely seen, and no differences exist between stimulated and control muscles. However, these observations do not exclude microinjuries at the ultrastructural level. Moreover, desmin immunoreactivity appears to be uniformly distributed within fibers and is elevated in stimulated muscles (Fig. 2). This may be viewed as an adaptive response to increased contractile activity, possibly enhancing tensile strength, also indicating that CLFS-induced changes occur at the level of structural elements encompassing the muscle's series elastic component. This finding is not surprising because slow fibers are known to have wider Z-discs, more desmin, and are exposed to greater chronic loads than are fast fibers (29).

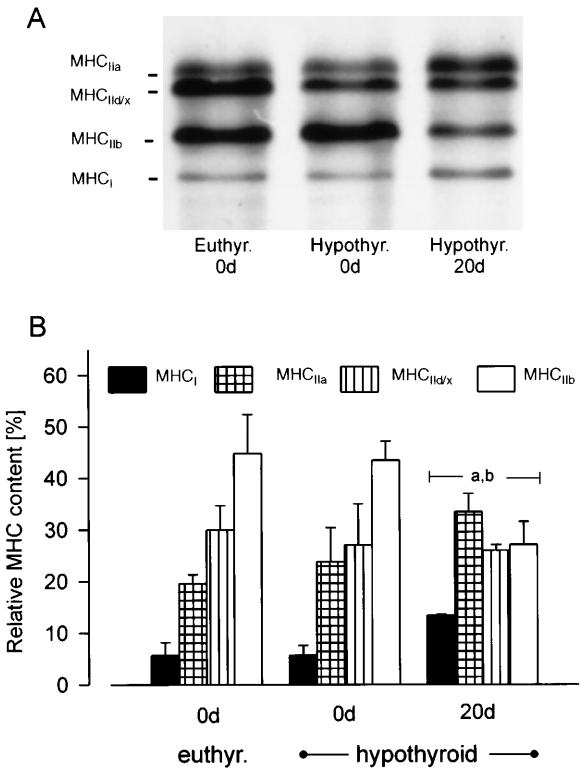

Fig. 12. Changes in electrophoretically determined MHC protein content after 20 days of CLFS. *A*: representative MHC gel; *B*: relative concentrations of MHC isoforms as evaluated by densitometry. [a] Different from euthyroid control; [b] different from hypothyroid control ($P < 0.05$).

The failure to detect morphological signs of fiber degeneration in chronically stimulated rat muscle is remarkable in comparison with rabbit muscle where degeneration/regeneration processes are pronounced (14, 16). This difference may be explained by the higher aerobic-oxidative metabolic potential of rat fast-twitch muscle, which, therefore, is better endowed for sustained contractile activity than is rabbit muscle. Consequently, when similar stimulation protocols are applied to both species, rabbit muscle responds by fiber transformation and replacement of fibers, deteriorated as a consequence of a metabolically induced myopathology. In contrast, rat muscle only responds by a transformation of existing fibers.

Satellite cells. The method used to identify satellite cells relates to their location between basal lamina and sarcolemma (36). Thus their identification was limited only to those cells clearly located between both the

immunocytochemically identified basal lamina and sarcolemma. Those few cells that could not be identified unambiguously, were not included. In addition, satellite cells detached from their original bed were also not counted.

According to our observations, satellite cells increase in number in the stimulated rat muscle fibers. Studies with BrdU labeling in vivo, showing an approximately fivefold increase in the number of labeled cells, unambigously prove that this increase results from enhanced proliferation (unpublished observations). This increase coincides with an even greater increment in intrafiber nuclei. The percentage of satellite cells, as referred to total intrafiber nuclei, increases from an average 3.8% in the euthyroid control to 13.8% in the 20-day-stimulated hypothyroid muscle (Fig. 8). This latter value is almost twofold higher than reported for the normal slow-twitch soleus muscle of rat (6.9%) (26). This comparison is justified, as the value given by these authors for normal EDL muscle (3.4%) is similar to that of our euthyroid control. Because the increase in the number of intrafiber nuclei is about threefold higher than the increase in satellite cells during the 20 days of CLFS, we suggest that satellite cells expand the satellite cell population and, in addition, fuse to existing fibers, thus augmenting their myonuclear density. It is obvious, however, that although the latter effect is consistent with the higher myonuclear density of normal slow fibers, this observation does not allow us to conclude on the role of satellite cells in fiber-type transitions.

Satellite cell activation has been shown to occur in response to various protocols of enhanced contractile activity, e.g., short-term high-intensity exercise training, endurance training, stretch-induced hypertrophy, and compensatory hypertrophy (see Ref. 27 for review). In this context, CLFS can be considered as a highly standardized and reproducible protocol of maximum endurance training. Therefore, any changes induced in the stimulated muscles represent maximum adaptive responses. Most relevant to the present study is the model of the myotonic ADR mouse in which, concomitant with enhanced neuromuscular activity, muscles display an elevated satellite cell content in the absence of fiber degeneration (23).

A remarkable finding is the pronounced and progressive upregulation of the MHC_{dev} in hypothyroid-stimulated muscles (Figs. 9 and 11). Approximately 60% of the fibers in 20-day-stimulated EDL muscles exhibit reactivity for the MHC_{dev} isoform. As judged from their large size, these fibers are preexisting fibers. This suggestion also applies to the 5-day-stimulated muscles in which regenerating fibers should be distinguishable by size from preexisting fibers. Transient expression of embryonic and/or neonatal myosin has also been observed in overloaded rat muscle in preexisting fibers (6, 34). However, models of compensatory hypertrophy typically display evidence of muscle degeneration/regeneration (31), making it difficult to separate the effects of muscle adaptation from experimentally induced fiber injury.

The expression of developmental myosin isoforms (MHC_{emb} and MHC_{neo}) in existing adult fibers of low-frequency-stimulated muscle is a novel finding, especially since fiber degeneration/regeneration processes were excluded by morphological criteria and the failure to detect vimentin in the fibers. This observation strongly points to a partial recapitulation of the myogenic program during the adaptive response. The appearance of MHC_{emb} and MHC_{neo} in low-frequency-stimulated rat muscle has obviously escaped detection by electrophoretic analyses of MHC isoform patterns. This applies also to the present study and is explained by incomplete separation of MHC_{emb} from MHC IIa and MHC IId(x), as well as of MHC_{neo} from MHC IIb, especially if these developmental isoforms are expressed at low levels. The finding that CLFS does not lead to decreases in the relative concentration of MHC IId/x (Fig. 12) might be due to comigration of upregulated developmental myosins. In this context, it should be clear that our immunohistochemical findings are qualitative and do not provide information as to the relative concentrations of the various MHC isoforms.

In dog diaphragm, also devoid of fiber necrosis during CLFS, embryonic MHC expression was not found (10). In contrast to that work, in which an antibody specific to only embryonic MHC was used, the antibody applied in the present study recognizes both the embryonic and neonatal MHC isoforms (20). An expression of an embryonic MHC isoform at the mRNA level has previously been observed in soleus muscle of the hypothyroid rat (11). Because no fiber type distribution was conducted in that study, it remains uncertain whether MHC_{emb} expression occurred in type I fibers or accompanied the type IIA-to-type I fiber transition induced by hypothyroidism. Interestingly, an upregulation of neonatal myosin has been shown in denervated rat muscle but was restricted to the type IIA fiber population (21). With regard to the present study, it is evident that the expression of MHC_{dev} primarily correlates with the expression of MHC IIa. MHC_{dev} seems to be first upregulated mainly in type IIA fibers and, with ongoing CLFS, is observed also in hybrid fibers transforming into type IIA. Therefore, the hybrid fiber population coexpressing MHC IIa, MHC I, and MHC_{dev} expands before the population of hybrid fibers displaying coexpression of MHC_{fast} with MHC IIa and MHC_{dev}. Transformation of fast fibers originally expressing MHC IIb and/or MHC IId/x would thus start to upregulate MHC_{dev} only when they reach the MHC IIa expression state during their fast-to-slow transition.

A possible explanation of the combined expression of MHC IIa and MHC_{dev} could be the tandem organization of the two corresponding genes (35). An alternate explanation might be derived from the similar time courses of increases in satellite cells, total myonuclei, and increases in MHC_{dev}-expressing fibers. These changes seem to be coordinated, suggesting that the addition of new nuclei to existing fibers induces or

facilitates the expression of the MHC_{dev} isoform. It could be that the MHC IIa state requires a certain myonuclear density. This idea may be extended to the next step, namely, that the ultimate MHC IIa-to-MHC I transition also depends on a high myonuclear density as a prerequisite for the last step in the fast-to-slow transformation. In this context, the question may be asked whether CLFS does not only increase the number of satellite cells but also changes their phenotypic properties. Although our results cannot answer this question, recently published observations on in vitro cultivated satellite cells from rabbit muscles exposed to long-term low-frequency stimulation argue against this possibility (1).

In summary, a fast-to-slow transition is induced by CLFS in hypothyroid rat muscle without macroscopic signs of degeneration/regeneration processes. The stimulation-induced fiber type conversion, therefore, exclusively results from the transformation of preexisting fibers. Fiber-type transformation encompasses an enhanced expression of desmin, indicating that CLFS also leads to a reorganization of cytoskeletal elements related to tensile strength. The fast-to-slow transitions are mirrored by the downregulation of the fast and the upregulation of slower myosin isoforms, the latter being accompanied by an induction of developmental isoforms. Furthermore, the number of satellite cells increases in the transforming fibers, attaining an almost twofold higher level than in normal slow-twitch soleus muscle. Coordinate increases in satellite cell and myonuclear contents indicate that some of the activated satellite cells fuse with existing fibers, thereby augmenting their myonuclear density even beyond that of normal slow fibers.

The authors thank I. Traub and E. Leisner for excellent technical assistance, and Prof. S. Schiaffino for providing the MHC antibodies.

This study was supported by the Deutsche Forschungsgemeinschaft Sonderforschungsbereich 156. C. T. Putman is a Fellow of the Canadian Medical Research Council and Muscular Dystrophy Association.

Address for reprint requests: D. Pette, Faculty of Biology, Univ. of Constance, D-78457 Constance, Germany (E-mail: Dirk.Pette@uni-konstanz.de).

Received 7 April 1998; accepted in final form 4 September 1998.

REFERENCES

1. **Barjot, C., P. Rouanet, P. Vigneron, C. Janmot, A. d'Albis, and F. Bacou.** Transformation of slow- or fast-twitch rabbit muscles after cross-reinnervation of low frequency stimulation does not alter the in vitro properties of their satellite cells. *J. Muscle Res. Cell Motil.* 19: 25–32, 1998.
2. **Bornemann, A., and H. Schmalbruch.** Desmin and vimentin in regenerating muscles. *Muscle Nerve* 15: 14–20, 1992.
3. **Brown, J. G., and D. J. Millward.** Dose response of protein turnover in rat skeletal muscle to triiodothyronine. *Biochim. Biophys. Acta* 757: 182–190, 1983.
4. **Darr, K. C., and E. Schultz.** Hindlimb suspension suppresses muscle growth and satellite cell proliferation. *J. Appl. Physiol.* 67: 1827–1834, 1989.
5. **Delp, M. D., and D. Pette.** Morphological changes during fiber type transitions in low-frequency stimulated rat fast-twitch muscle. *Cell Tissue Res.* 277: 363–371, 1994.
6. **Dunn, S. E., and R. N. Michel.** Coordinated expression of myosin heavy chain isoforms and metabolic enzymes within overloaded rat muscle fibers. *Am. J. Physiol.* 273 (*Cell Physiol.* 42): C371–C383, 1997.
7. **Düsterhöft, S., and D. Pette.** Satellite cells from slow rat muscle express slow myosin under appropriate culture conditions. *Differentiation* 53: 25–33, 1993.
8. **Gibson, M. C., and E. Schultz.** The distribution of satellite cells and their relationship to specific fiber types in soleus and extensor digitorum longus muscles. *Anat. Rec.* 202: 329–337, 1982.
9. **Goebel, H. H.** Desmin related neuromuscular disorders. *Muscle Nerve* 18: 1306–1320, 1995.
10. **Hoffman, R. K., B. Gambke, L. W. Stephenson, and N. A. Rubinstein.** Myosin transitions in chronic stimulation do not involve embryonic isozymes. *Muscle Nerve* 8: 796–805, 1985.
11. **Izumo, S., B. Nadal-Ginard, and V. Mahdavi.** All members of the MHC multigene family respond to thyroid hormone in a highly tissue-specific manner. *Science* 231: 597–600, 1986.
12. **Jaschinski, F., M. Schuler, H. Peuker, and D. Pette.** Transitions in myosin heavy chain mRNA and protein isoforms of rat muscle during forced contractile activity. *Am. J. Physiol.* 274 (*Cell Physiol.* 43): C365–C371, 1998.
13. **Kirschbaum, B. J., H.-B. Kucher, A. Termin, A. M. Kelly, and D. Pette.** Antagonistic effects of chronic low frequency stimulation and thyroid hormone on myosin expression in rat fast-twitch muscle. *J. Biol. Chem.* 265: 13974–13980, 1990.
14. **Lexell, J., J. Jarvis, D. Downham, and S. Salmons.** Quantitative morphology of stimulation-induced damage in rabbit fast-twitch skeletal muscles. *Cell Tissue Res.* 269: 195–204, 1992.
16. **Maier, A., B. Gambke, and D. Pette.** Degeneration-regeneration as a mechanism contributing to the fast to slow conversion of chronically stimulated fast-twitch rabbit muscle. *Cell Tissue Res.* 244: 635–643, 1986.
17. **Norenburg, K. M., R. A. Herb, S. L. Dodd, and S. K. Powers.** The effects of hypothyroidism on single fibers of rat soleus muscle. *Can. J. Physiol. Pharmacol.* 74: 362–367, 1996.
18. **Pette, D., and R. S. Staron.** Mammalian skeletal muscle fiber type transitions. *Int. Rev. Cytol.* 170: 143–223, 1997.
19. **Pette, D., and G. Vrbová.** Adaptation of mammalian skeletal muscle fibers to chronic electrical stimulation. *Rev. Physiol. Biochem. Pharmacol.* 120: 116–202, 1992.
20. **Picquet, F., L. Stevens, G. S. Butler-Browne, and Y. Mounier.** Contractile properties and myosin heavy chain composition of newborn rat soleus muscles at different stages of postnatal development. *J. Muscle Res. Cell Motil.* 18: 71–79, 1997.
21. **Schiaffino, S., L. Gorza, G. Pitton, L. Saggin, S. Ausoni, S. Sartore, and T. Lömo.** Embryonic and neonatal myosin heavy chain in denervated and paralysed rat skeletal muscle. *Dev. Biol.* 127: 1–11, 1988.
22. **Schiaffino, S., L. Gorza, S. Sartore, L. Saggin, S. Ausoni, M. Vianello, K. Gundersen, and T. Lömo.** Three myosin heavy chain isoforms in type 2 skeletal muscle fibres. *J. Muscle Res. Cell Motil.* 10: 197–205, 1989.
23. **Schimmelpfeng, J., H. Jockusch, and P. Heimann.** Increased density of satellite cells in the absence of fibre degeneration in muscle of myotonic mice. *Cell Tissue Res.* 249: 351–357, 1987.
24. **Schuler, M., and D. Pette.** Fiber transformation and replacement in low-frequency stimulated rabbit fast-twitch muscles. *Cell Tissue Res.* 285: 297–303, 1996.
25. **Schultz, E.** A quantitative study of satellite cells in regenerated soleus and extensor digitorum longus muscles. *Anat. Rec.* 208: 501–506, 1984.
26. **Schultz, E., and K. C. Darr.** The role of satellite cells in adaptive or induced fiber transformations. In: *The Dynamic State of Muscle Fibers*, edited by D. Pette. Berlin: de Gruyter, 1990, p. 667–679.
27. **Schultz, E., and K. M. McCormick.** Skeletal muscle satellite cells. *Rev. Physiol. Biochem. Pharmacol.* 123: 213–257, 1994.
28. **Simoneau, J.-A., and D. Pette.** Species-specific effects of chronic nerve stimulation upon tibialis anterior muscle in mouse, rat, guinea pig, and rabbit. *Pflügers Arch.* 412: 86–92, 1988.

29. **Small, J. V., D. O. Fürst, and L. E. Thornell.** The cytoskeletal lattice of muscle cells. *Eur. J. Biochem*. 208: 559–572, 1992.
30. **Snow, M. H.** Satellite cell response in rat soleus muscle undergoing hypertrophy due to surgical ablation of synergists. *Anat. Rec.* 227: 437–446, 1990.
31. **Tamaki, T., A. Akutsuka, M. Y. Tokunga, S. Uchihama, and T. Shiraisi.** Characteristics of compensatory hypertrophied muscle in the rat: I. Electron microscopic and immunohistochemical studies. *Anat. Rec.* 246: 325–335, 1996.
32. **Termin, A., R. S. Staron, and D. Pette.** Changes in myosin heavy chain isoforms during chronic low-frequency stimulation of rat fast hindlimb muscles—a single fiber study. *Eur. J. Biochem*. 186: 749–754, 1989.
33. **Vater, R., M. J. Cullen, and J. B. Harris.** The expression of vimentin in satellite cells of regenerating skeletal muscle in vivo. *Histochem. J*. 26: 916–928, 1994.
34. **Yang, H., M. Alnaqeeb, H. Simpson, and G. Goldspink.** Changes in muscle fibre type, muscle mass and *IGF-1* gene expression in rabbit skeletal muscle subjected to stretch. *J. Anat.* 190: 613–622, 1997.
35. **Yoon, S. J., S. H. Seiler, R. Kucherlapati, and L. Leinwand.** Organization of the human skeletal myosin heavy chain gene cluster. *Proc. Natl. Acad. Sci. USA* 89: 12078–12082, 1992.
36. **Zhang, M., and I. S. McLennan.** Use of antibodies to identify satellite cells with a light microscope. *Muscle Nerve* 17: 987–994, 1994.